ELSEVIER

International Journal of Mass Spectrometry 215 (2002) 101–111

International Journal of Mass Spectrometry

www.elsevier.com/locate/ijms

Active pixel sensors for mass spectrometry

Stephen Fuerstenau*, George Soli[1], Thomas Cunningham, Bruce Hancock, Bedabrata Pain, Mahadeva Sinha

Jet Propulsion Laboratory, California Institute of Technology, Pasadena, CA 91109, USA

Received 22 August 2001; accepted 20 November 2001

Abstract

Active pixel sensors (APS) are micro-fabricated CMOS amplifier arrays that are rapidly replacing CCD devices in many electronic imaging applications. Unlike the pixels of a CCD device, the sensing elements of the APS will respond to locally situated electrostatic charge, owing to the amplifier present in each pixel. We have built two small test arrays with microscopic aluminum electrodes integrated onto standard APS readout circuitry for the purpose of detecting low-energy gas-phase ions in mass spectrometers and other analytical instruments. The devices exhibit a near-linear dynamic range greater than four orders of magnitude, and a noise level of less than 100 electrons at room temperature. Data are presented for the response of the APS detectors to small ions in a miniature magnetic sector mass spectrometer and in an atmospheric pressure jet of helium. Data for individual highly-charged electrospray droplets are presented as well. Anticipated improvements suggest that in the near future APS ion detectors will posses noise levels approaching 10 electrons and will have a useful dynamic range over six orders of magnitude. (Int J Mass Spectrom 215 (2002) 101–111) © 2002 Elsevier Science B.V. All rights reserved.

Keywords: Array detector; Charge; Mass spectrometry; CMOS; Faraday cup

1. Introduction

This paper reports preliminary results of the application of complimentary metal oxide semiconductor (CMOS) imaging technology to the detection of gas-phase ions. Over the past decade, substantial progress has been made, at JPL and elsewhere, in the use of CMOS devices for scientific imaging applications [1,2].

Although, it is traditionally used for digital applications, CMOS technology has been adapted to function in low-level analog signal sensing applications. The benefits of this development are numerous. CMOS imaging devices require just 1% of the power consumed in charge coupled imaging chips (CCDs). The chips are relatively inexpensive to manufacture and permit integration of sensing, control, and signal digitization circuitry on the same piece of silicon. Such 'camera-on-a-chip' imaging devices are now commercially available.

The primary difference between CMOS image sensors and CCDs is the presence of an amplifier in each pixel. In a CCD, charge is generated and trapped by the capture of photons inside the doped silicon pixel wells and then 'pushed' through the silicon matrix from one pixel to another, until it is measured at the edge of the array by a single amplifier. Such amplifiers can be made to sense just a few electrons [3]. When an

* Corresponding author.
E-mail: stephen.d.fuerstenau@jpl.nasa.gov
[1] Present address: Integrated Detector Systems, Vancouver, WA 98668, USA.

1387-3806/02/$20.00
PII S1387-3806(01)00589-9

electrostatic charge is placed on the surface of a pixel, it induces an image charge in that pixel which can be sensed. However, unlike the free charges that are normally created within a CCD by energetic photons, this image charge cannot be transported away from the surface charge that induces it. As a consequence, a CCD device will not respond to charge deposited on the surface of its pixels. This capability is desirable, however, for looking at low-energy ions or larger, more energetic ions moving at low velocities. CCDs have been used to detect relatively high-energy (5 kV) low-mass ions in an imaging secondary ion mass spectrometer [4]. In those experiments the ions were moving with enough speed to liberate electrons within the bulk silicon of the pixel upon impact. These electrons could then be sensed in the normal manner. At lower kinetic energy or higher mass ($m > 100$ amu), the detection efficiency of the CCD detector quickly dropped to zero.

In contrast to CCDs, CMOS imaging devices possess an amplifier in each pixel, and hence are commonly referred to as active pixel sensors (APS). Such pixels will respond to charge deposited locally on their surfaces by sensing the image charge induced by it. In an imaging APS device the pixels contain a light-sensitive, doped silicon region that is biased relative to the input of an FET so as to form a photodiode or photo-gate. For the purpose of detecting ions the pixels are slightly modified by replacing the light-sensitive region with a bare metal electrode directly connected to the gate of the FET. The capacitance to ground of such an electrode can be made as low as a few femtofarads, leading to measurable voltage changes from the presence of very small quantities of charge. It is the small capacitance of the pixels that is responsible for the remarkable sensitivity of APS devices. For example, an electrode with a capacitance of 10 fF and a charge of 10 electrons will have its potential raised by 100 μV, which is the level of voltage noise that is typically encountered during readout operation. In our laboratory, APS imagers have exhibited noise levels under 10 electrons at room temperature [5].

Most imaging devices operate in a sample and hold readout mode. Charge is integrated for a precise time duration and then sampled for a time that is on the order of microseconds or less. Typically, this operation is carried out in a rolling sequential fashion, i.e., one pixel is read out while the rest are integrating the signal. Large format arrays (512×512) can be read out at several frames per second. While such frame rates do allow for quasi-continuous ion monitoring, APS based detectors cannot currently be used for time-of-flight applications. The intrinsic sensing precision of the APS measurement is limited by kTC noise which is related to 'Johnson' noise. It is associated with thermally induced variations of the pixel reset level voltage, VDD. This noise source can be greatly reduced if the reset level is sampled prior to integration. The technique, known as correlated double sampling, amounts to reading each pixel twice per frame and is commonly employed for low noise applications.

2. APS ion detectors

Our motivation of exploring the use of APS technology for detecting ions was two-fold. Initially we were interested in developing techniques for determining the charge on massive electrospray ions by charge detection mass spectrometry (CDMS) [6]. In this technique, the mass of electrospray ions is assessed by measuring both the mass-to-charge ratio (m/z) and the charge for individual ions possessing hundreds or thousands of charges. Using this approach we have 'weighed' megadalton DNA samples as well as nano-particles and intact virus ions [7,8]. In those experiments we passed the ion beam through a Faraday cage electrode about 3 cm in length. The charge sensitive preamplifier we employed for that instrument had a minimum noise level of about 50–100 electrons due to the 5 pF capacitance of the electrode. This capacitance could only be reduced at the expense of reducing the detector cross-section. We speculated that an array of microscopic Faraday cups might provide a means for lower noise measurement, owing to

the small capacitance of each cup, while still providing an overall target area useful for ion collection. In this application, the position of the ion is not important, and the array strategy is analogous to covering a barn door with bull's-eyes. The 28 × 28 array described below was developed to test this hypothesis. Matsumoto and co-workers developed a similar detector technology for imaging beams of singly charged ions in a secondary ion mass spectrometer [9]. That device had 15 μm pixel dimensions, was operated at −127 °C, and achieved a noise level of about 25 electrons per pixel. A second application of interest to us is a low-power, compact array detector for use in a miniature Mattauch–Herzog magnetic sector instrument developed at JPL [10]. The focal plane region of the instrument is 30 mm long with a magnet gap of

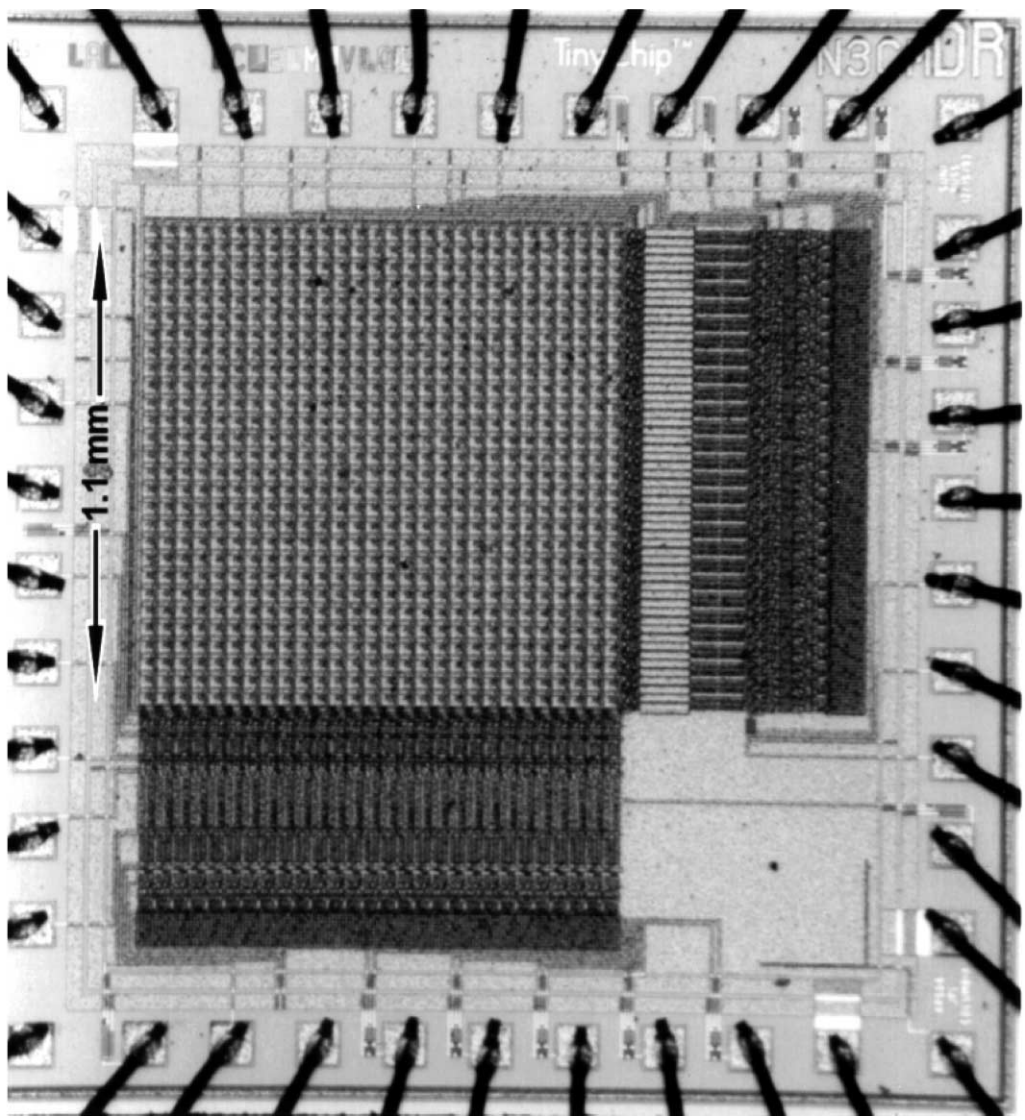

Fig. 1. A 28 × 28 array of metal plate electrodes fabricated with CMOS technology. This test array has dimensions of 1.1 mm, but centimeter size formats are possible.

3 mm. The 128 pixel linear array described below was developed for testing with that instrument.

The chips were designed using software tools at JPL and then submitted to a commercial CMOS foundry for fabrication through the MOSIS prototyping service organization (Information Sciences Institute, University of Southern California, Marina del Rey, CA). This service allows a set of prototype chips (usually 25) to be purchased for an amount based on the chip area, but significantly less than the cost of an entire lot run. A photograph of this 2D array device is given in Fig. 1. The detector is comprised of 784 metal pixels, each $36\,\mu m^2$ on a $40\,\mu m$ pitch. Row and column address circuitry is visible at the side of the chip, and is passivated with a layer of undoped poly-crystalline silicon. During testing all but the array portion of the detector was protected from ion bombardment by a metal foil mask with a 1 mm window. A detail of a pixel from this detector is illustrated in Fig. 2. The surface layer that forms the electrode is aluminum and appears darker than the surrounding silicon in the SEM micrograph. When a highly-charged ion or particle lands on a metal pixel, charge will flow off of it to the pixel if the particle is conductive. If the particle is of a non-conductive material, the charge will remain on it but will be balanced by a flow of image charge onto the pixel when the potential is reset. This charge will balance the immobile charge residing on the pixel so that the electrode will appear uncharged to approaching ions.

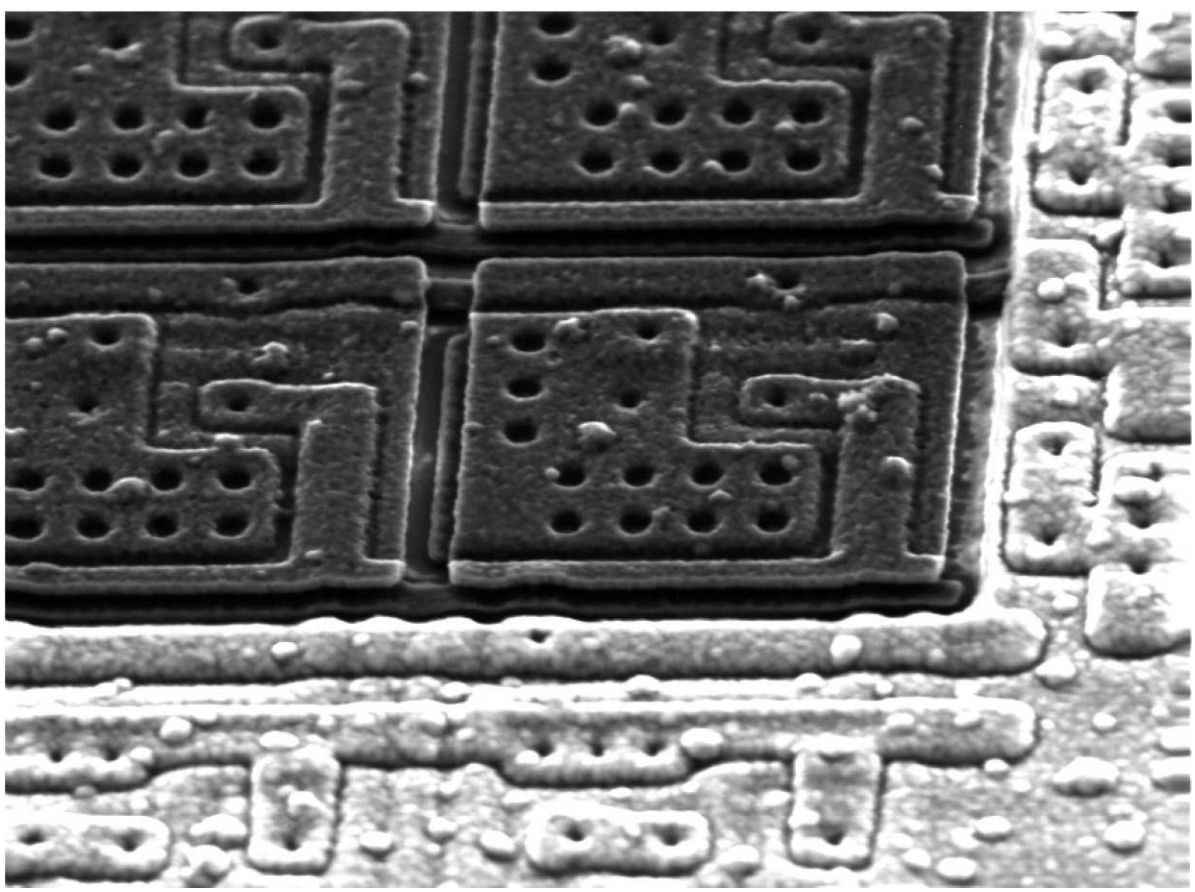

Fig. 2. A $36\,\mu m$ metal electrode at the corner of the 28×28 pixel array. This pixel will respond to a charged particle by changing its potential in proportion to the level of charge and inversely to its capacitance. The ground to plate capacitance of the pixel is estimated to be 15 fF.

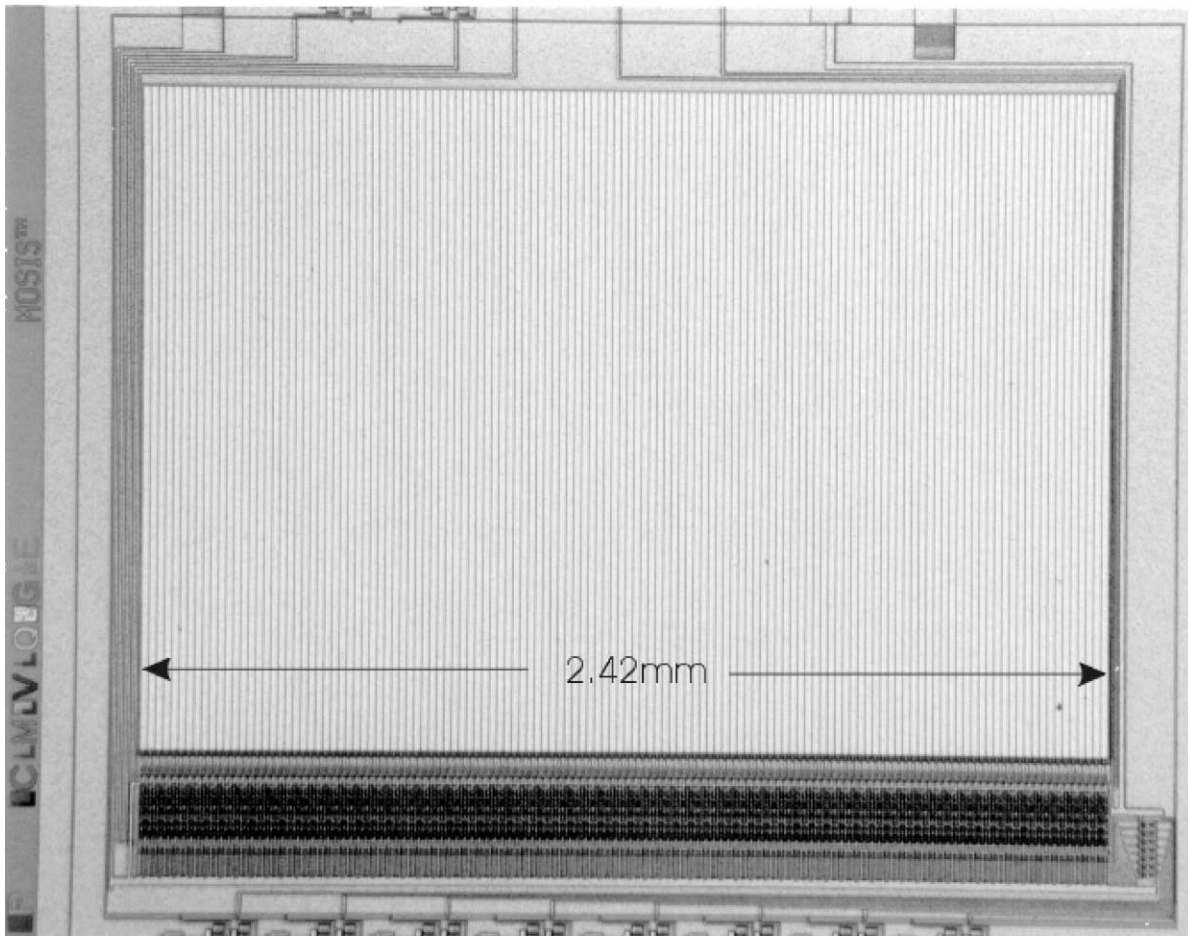

Fig. 3. A 128 linear array of metal strip electrodes, each connected to a CMOS transistor and multiplexed readout. The aluminum strip pixels are 16 μm wide and arrayed on a 20 μm pitch. Each pixel measures 1600 μm in length.

A second APS detector of a linear design consisting of 128 metal strip electrodes is illustrated in Figs. 3 and 4. The aluminum strips are 16 μm wide × 1600 μm long, and are arrayed on a 20 μm pitch. The capacitance to ground of each pixel is estimated to be 0.3 pF.

3. APS pixel design and readout

The pixel unit cell consists of a metal electrode plate, a source-follower input transistor, a row-selection transistor and a row-reset transistor, as illustrated in Fig. 5. At the bottom of each column of pixels, there is a load transistor VLN and two output branches to store the reset and signal levels. Each branch consists of a sample and hold capacitor (CS or CR) with a sampling switch (SHS or SHR) and a second source-follower with a column-selection switch (COL).

The reset and signal levels are read out differentially, to remove non-uniformity in level offset (but not kTC noise) from the pixel. If the signal levels are read out twice, once before integration and once after integration, kTC noise is also suppressed. These readout circuits are common to an entire column of pixels. The

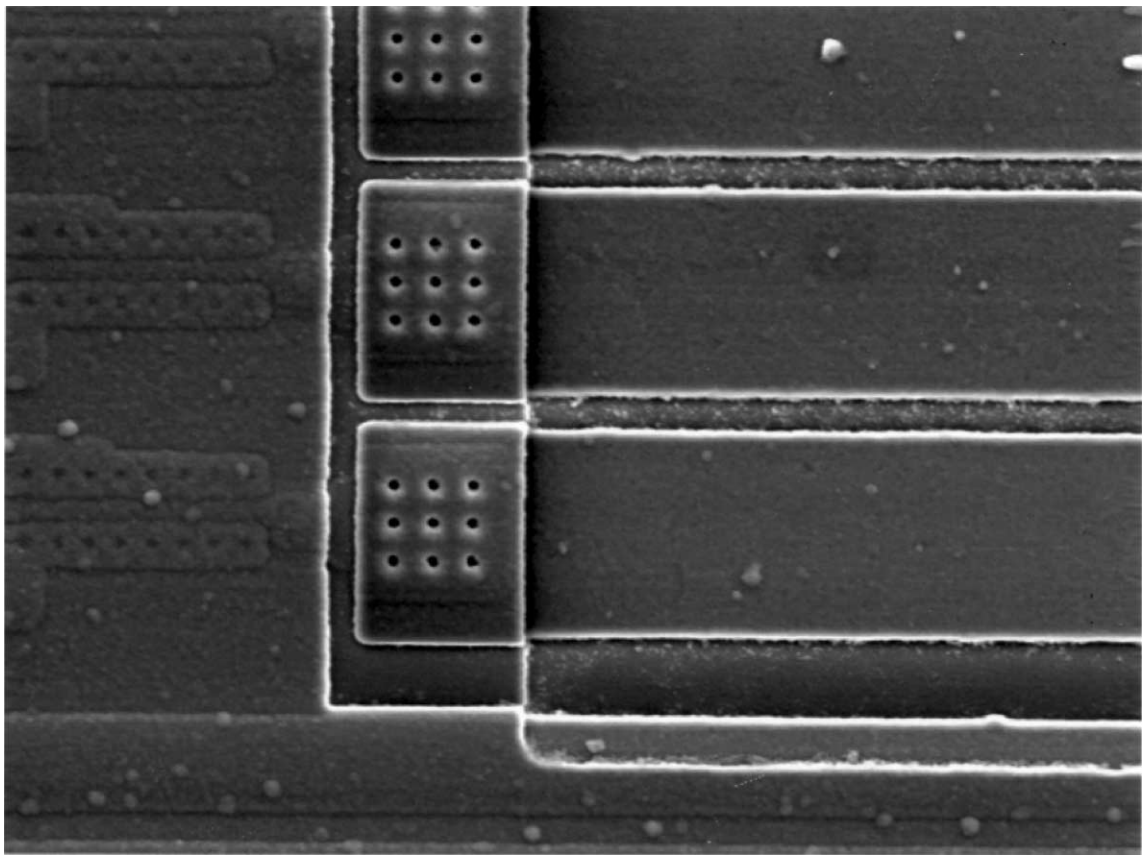

Fig. 4. Micrograph illustrating detail of the 16 μm wide strip electrodes.

load transistors of the second set of source-followers (VLP) are common to the entire array. In operation a row is selected and the signal level V_2 is stored on CS. The row is then reset and reset level V_3 is stored on CR. Each column is then read out through a differential amplifier giving (V_2–V_3). This voltage difference can be recorded and a new row selected or stored in memory for kTC noise suppression. For kTC noise suppression the row must be read out twice for each reset. The row is reset and signal level V_1 is read without using CS or measuring the reset level. The row pixels integrate charge and signal level V_2 is read out giving a (V_2–V_1) signal level suppressing kTC noise. These signal and reset voltages are shown in Fig. 6. The voltage (V_2–V_1) is then recorded. This operation does not use CR or CS. For typical on-chip capacitor designs the CR and CS kTC noise is about 1/3 of the noise without pixel kTC noise suppression.

4. Initial ion detection results

Charged droplets of polyethylene glycol/methanol solution were created with an electrospray ion source and accelerated with a 300 V potential in a free jet vacuum interface of a charge detection mass spectrometer [6]. A fraction of the ions in the beam traveled through a cylindrical Faraday cage electrode, registering as pulses whose heights were proportional to the droplet's charge. The charge distribution on those droplets, as measured by this technique, had a mean charge of 1680 ± 150 electrons. A fraction of the

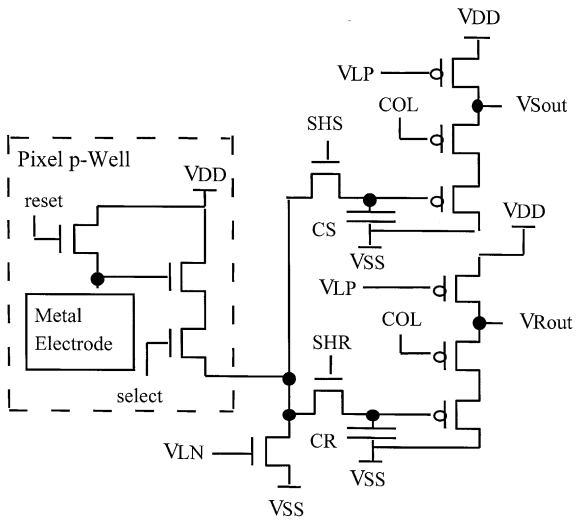

Fig. 5. CMOS Faraday-cup pixel circuit schematic showing pixel, with row-reset and row-select, and column sample and hold capacitors and output circuitry.

droplets that were detected in the cylindrical electrode struck the APS detector. The mean charge states measured by both detectors were equated and formed the basis for calibration of the APS detector.

During a row read cycle, image charge potentials were stored on the column signal capacitors. The row pixels were then reset and the reset potentials were stored on the column reset capacitors. The row-reset transistors were then turned off and the row of pixel's integrated charge for 1.5 s before repeating the row read cycle. The difference between the row pixels signal and reset potentials was then measured with a

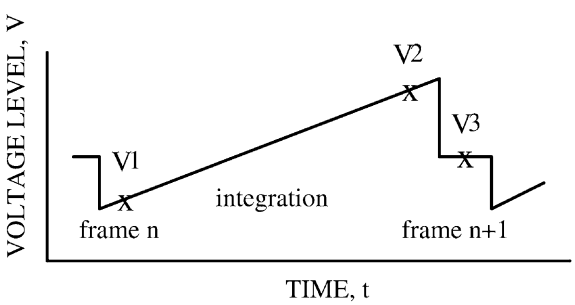

Fig. 6. Voltage level diagram showing reset level V_3 and signal levels V_1 and V_2 as a function of time.

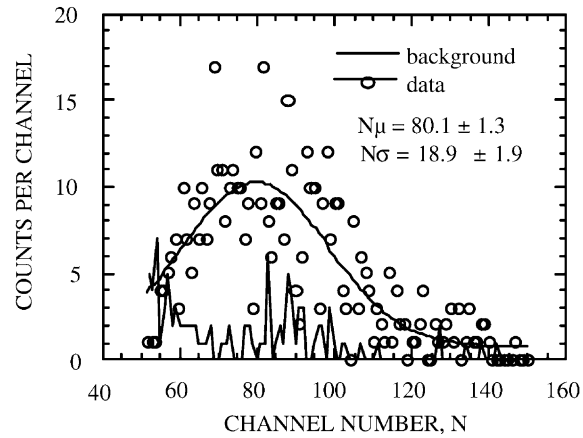

Fig. 7. Distribution of charged droplets with a mean charge of 1680 electrons in channel 80, with 21 electrons per channel.

differential op-amp. The data were collected in 599 frames over 16 min (about 1.6 s per frame) with 569 frames containing data above a threshold set at channel 50. The data set summarized in Fig. 7 was collected in 603 frames with 205 frames containing background data.

The background noise indicated was caused by the asynchronous chip operation with the CAMAC digital output. The reset pulse was held for a fluctuating number of CAMAC clock cycles causing the reset level to fluctuate. This problem can be overcome by not measuring the reset level and histogramming (V_2–V_1) as shown in Fig. 8. This mode of operation also suppresses kTC noise as described previously and measures a read noise floor plus dark current of 90 electrons rms at room temperature. These dark current electrons can be removed by cooling or by making several measurements around V_1 and V_2 and averaging. The remaining 85 electrons rms read noise was attributed to process parameters and could be reduced by circuit design.

The linear strip array was mounted in the focal plane of the JPL miniature magnetic sector mass spectrometer. Ions generated from an air leak were focused onto the detector with an energy of 800 eV. The detector response is plotted in Fig. 9. The intensity profile is not indicative of the true resolution of

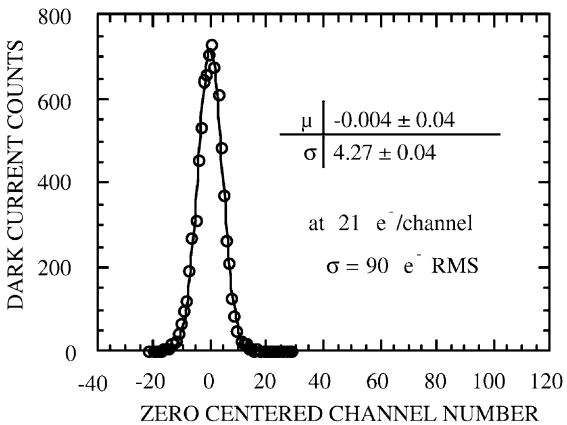

Fig. 8. Dark current histogram at room temperature showing an 90 electron rms noise.

the instrument but is instead a result of the imperfect alignment of the high-aspect ratio detector pixels with the vertical plane of the ion beam. The peak value of 60 mV represents a charge on that pixel of 110,000 electrons collected over a period of 20 ms. This corresponds to a current of about 1 pA for this pixel. The pixels were read out with a precision of under 200 μv corresponding to a noise level of less than 400 electrons. The data in Fig. 9 are the average of 25 frames, each frame integrated for 20 ms. The noise level associated with the baseline of the data is about 75 electrons.

An additional ion measurement experiment was carried out with the strip detector at atmospheric pressure. A 0.4 mm wide jet of helium was directed against the surface of the detector with a metal capillary nozzle positioned 2 mm away from the detector. A corona discharge was induced upstream of the nozzle causing positively charged helium ions to impinge on the pixels. The nozzle was biased with a few volts relative to the detector surface. These ions, therefore, reached the detector with thermal energies, proving that the ion induced response of the APS is a non-energetic process. Ion profiles are indicated in Fig. 10. The double-peak, axi-symmetric profile is consistent with an ion deposition that is a function of the shear rate of the impinging jet. At the jet center line the flow exhibits a stagnation point and ion deposition occurs without the benefit of a shear-thinned convective boundary layer. APS detectors should find use in ion mobility instruments as well, particularly those based on differential ion mobility in which a spatial separation of the ions is created. We have also been able to make this linear

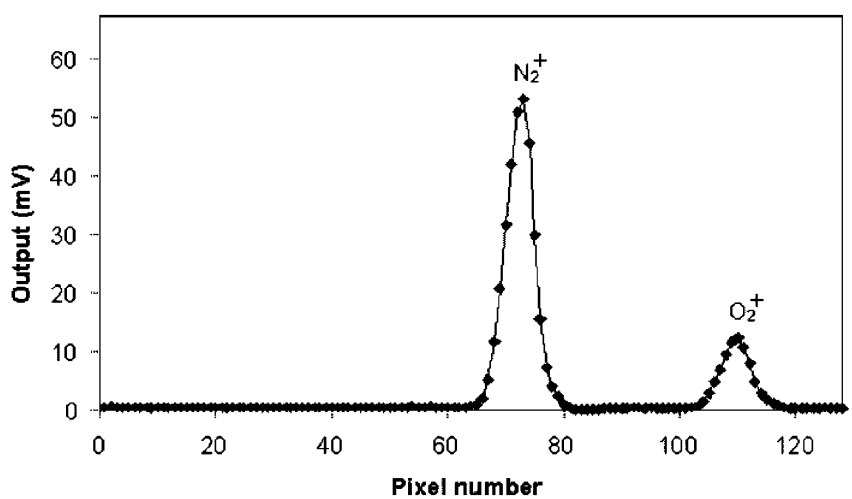

Fig. 9. Spectrum of air ions obtained with 128 pixel linear array in a miniature magnetic sector mass spectrometer. Peak flux for nitrogen ion is 1 pA collected at a single pixel.

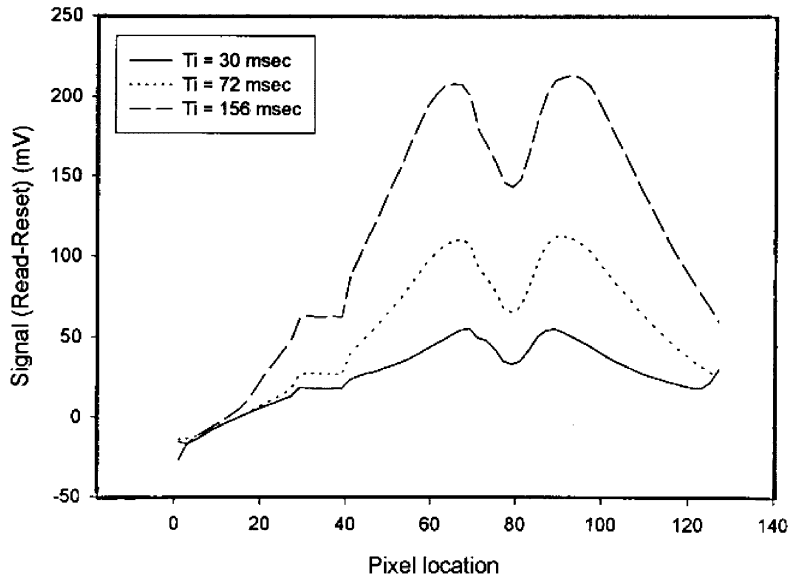

Fig. 10. Ion charging profiles from deposition of He+ ions in an atmospheric pressure jet of helium centered at pixel number 80 of the 128 pixel linear array. Profile shape is preserved over a range of integration times. The valley in the profile is consistent with reduced ion deposition at the stagnation point of the flow.

array detector respond to individual charged dust particles with a few thousand charges, although, the 2D array detector is better suited for this purpose.

5. Prospects for APS ion detectors

The reduction of readout noise is a primary goal of the APS detector development effort. Careful attention to timing circuitry should reduce noise associated with dark current fluctuations, as asynchronous triggering of the readout added significantly to the noise observed in the experiments with the 2D detector. One means for reducing noise is to add gain to the front end of the pixel amplifier string. Such a strategy should reduce the minimum detectable charge by a factor of 10, to around 15 electrons at room temperature, but only with a comparable reduction in the maximum charge carried by a pixel. The dynamic range of the detector is over 10,000–1, based on a full well pixel potential of 2500 mV and a noise level of 200 μV. At higher potentials pixel non-linearity is greater than a few percent. One strategy for increasing the dynamic range of the detector is the incorporation of a selective reset circuit. Each pixel is interrogated with a non-destructive read and is reset to the ground potential only when its charge level reaches a predetermined threshold. This approach prevents the build-up of kTC noise in pixels receiving low ion fluxes from unnecessary pixel reset operations. This strategy is not possible with CCDs as the readout in those devices is destructive by necessity.

We have demonstrated that the APS is a sensitive and versatile detector of gas-phase ions. The technology has benefited from the significant progress that has been made over the last decade in CMOS imaging devices. Fully integrated detector systems-on-a-chip have been realized in low power, low cost devices such as the camera illustrated in Fig. 11 [11]. We are also developing radiation hardened CMOS devices for space applications [12]. As these devices find further application as detectors for gas-phase ions and other particles, the full benefits of CMOS integrated circuit technology can be anticipated.

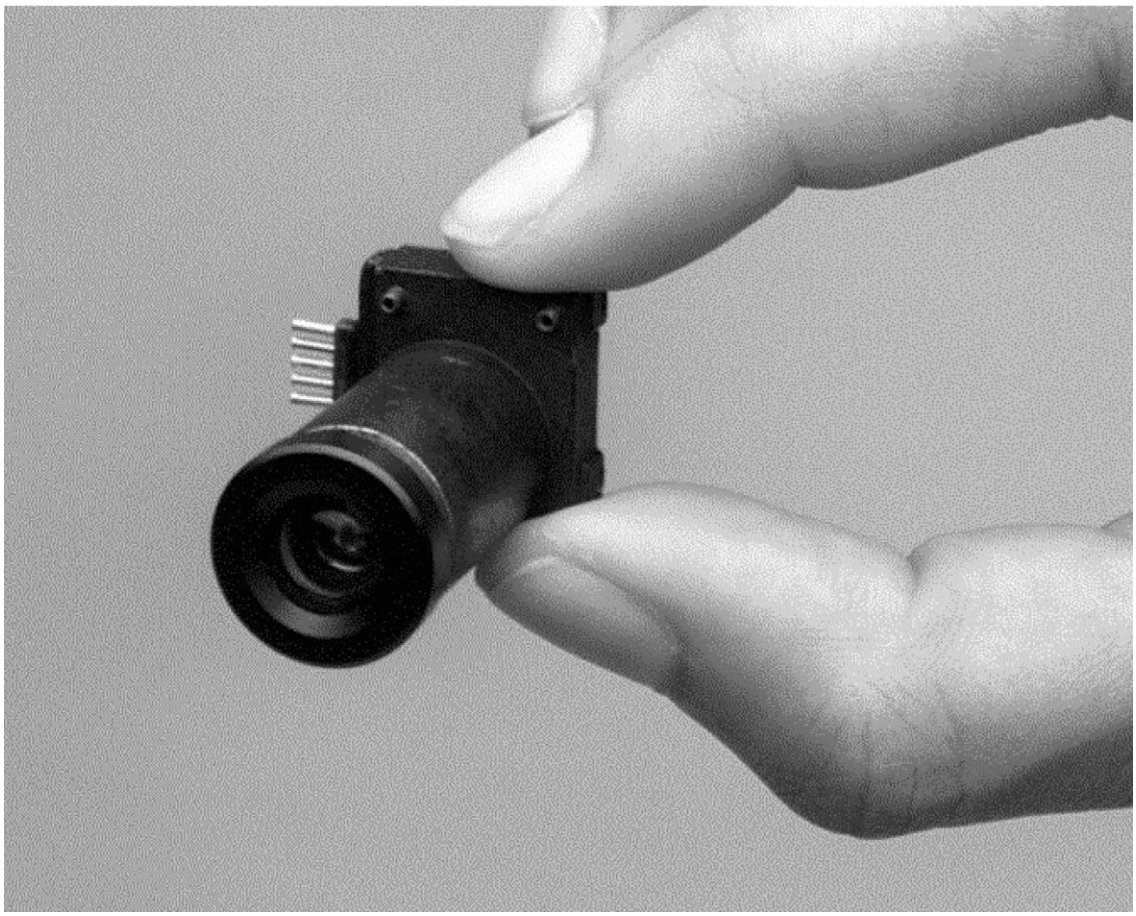

Fig. 11. The JPL single-chip camera with a 512 × 512 pixel focal plane array. The camera has complete on-chip control and analog to digital conversion circuitry.

References

[1] S. Mendis, S. Kemeny, E.R. Fossum, A 128 × 128 CMOS active pixel image sensor for highly integrated imaging systems, in: Proceedings of the International Electron Devices Meeting (IEDM) Technical Digest, Washington, DC, 5–8 December, 1993, pp. 583–586.

[2] E.R. Fossum, CMOS active pixel image sensors, Nucl. Istrum. Meth. A 395 (3) (Aug 21, 1997) 291–297.

[3] S. Ohsawa, Y. Matsunaga, Analysis of low signal level characteristics for high-sensitivity CCD charge detector, IEEE Trans. Electron Devices 39 (6) (1992) 1465–1468.

[4] L. Turner, D. Mantus, Y.C. Ling, M. Bernius, G. Morrison, Development and characterization of a charge-coupled device detection system for ion microscopy, Rev. Sci. Instrum. 60 (5) 1989.

[5] B. Pain, E.R. Fossum, Design and operation of self-biased high-gain amplifier arrays for photon-counting sensors in Infrared Readout Electronics III, Proc. SPIE, Vol. 2745, paper 08, 1996.

[6] S.D. Fuerstenau, W.H. Benner, Molecular weight determination of megadalton DNA electrospray ions using charge detection time-of-flight mass spectrometry, Rapid Commun. Mass Spec. 15 (1995) 1528–1538.

[7] S. Fuerstenau, W. Benner, Weighing intact virus particles with a charge detection mass spectrometer, in: Proceedings of the 44th ASMS Conference on Mass Spectrometry and Allied Topics, Portland, USA, 1996.

[8] S. Fuerstenau, W. Benner, J. Thomas, C. Brugidou, B. Bothner, G. Siuzdak, Mass spectrometry of an intact virus, Angew. Chem. Int. Ed. 40 (3) (2001) 541–544;
S. Fuerstenau, W. Benner, J. Thomas, C. Brugidou, B.

Bothner, G. Siuzdak, Mass spectrometry of an intact virus, Angew. Chem. Int. Ed. 40 (6) (2001) 9822–9822.

[9] K. Mtsumoto, H. Yurimoto, K. Kosaka, K. Miyata, T. Nakamura, S. Sueno, A novel ion imager for secondary ion mass spectrometry, IEEE Trans. Electron Devices 40 (1) (1993).

[10] M.P. Sinha, A miniature mass spectrometer for air quality measurement in space human habitat, J. Aerospace, Vol. 107, January 1999.

[11] B. Pain, G. Yang, B. Olson, T. Shaw, M. Ortiz, J. Heynssens, C. Wrigley, C. Ho, A low-power digital camera-on-a-chip implemented in CMOS active pixel approach, in: Proceedings of the 12th VLSI Design Conference, 7–9 January, 1999.

[12] C.C. Liebe, E.W. Dennison, B. Hancock, R.C. Stirbl, B. Pain, Active pixel sensor (APS) based star tracker, in: Proceedings of the IEEE Aerospace Conference, Aspen, March 1998.